Cell Death and Differentiation (2016) 23, 876–888

www.nature.com/cdd

The ubiquitin ligase Smurf2 suppresses TGFβ-induced epithelial–mesenchymal transition in a sumoylation-regulated manner

AS Chandhoke[1], K Karve[1], S Dadakhujaev[1,2], S Netherton[1,2], L Deng[1] and S Bonni*[,1]

Epithelial–mesenchymal transition (EMT) is a fundamental cellular process in epithelial tissue development, and can be reactivated in cancer contributing to tumor invasiveness and metastasis. The cytokine transforming growth factor-β (TGFβ) is a key inducer of EMT, but the mechanisms that regulate TGFβ-induced EMT remain incompletely understood. Here, we report that knockdown of the ubiquitin ligase Smurf2 promotes the ability of TGFβ to induce EMT in a three-dimensional cell culture model of NMuMG mammary epithelial cells. In other studies, we identify Smurf2 as a target of the small ubiquitin like modifier (SUMO) pathway. We find that the SUMO-E2 conjugating enzyme Ubc9 and the SUMO E3 ligase PIAS3 associate with Smurf2 and promote its sumoylation at the distinct sites of Lysines 26 and 369. The sumoylation of Smurf2 enhances its ability to induce the degradation of the TGFβ receptor and thereby suppresses EMT in NMuMG cells. Collectively, our data reveal that Smurf2 acts in a sumoylation-regulated manner to suppress TGFβ-induced EMT. These findings have significant implications for our understanding of epithelial tissue development and cancer.
Cell Death and Differentiation (2016) **23,** 876–888; doi:10.1038/cdd.2015.152; published online 18 December 2015

Epithelial–mesenchymal transition (EMT) is an essential process in epithelial tissue morphogenesis in the developing organism and contributes to postnatal events including mammary postnatal gland development as well as wound healing.[1,2] Importantly, EMT can be reactivated during cancer and may contribute to tumor invasiveness.[3] Epithelial cells undergoing EMT change phenotypically from cuboidal to fibroblastic morphology, lose epithelial markers including E-cadherin, gain mesenchymal markers, and display increased cell motility and invasiveness.[4,5] The secreted factor transforming growth factor-β (TGFβ) has emerged as a potent inducer of EMT with key roles in development and cancer.[6] Thus, there has been interest in the mechanisms that mediate TGFβ-induced EMT.

Smurf2 (Smad (Sma and mad) ubiquitination regulatory factor-2) is a HECT (for homology to E6 carboxy terminus domain)-containing E3 ubiquitin ligase that specifies substrates for ubiquitination and degradation by the proteasome.[7,8] Smurf2 regulates key biological processes during development and homeostasis including cell polarity, cell cycle, and senescence in an E3 ligase-dependent or -independent manner.[9–15] The biological functions of Smurf2 occur via regulation of signaling pathways including the TGFβ–Smad signaling pathway.[16–23] However, the role of Smurf2 in TGFβ-induced EMT has remained to be determined.

Sumoylation refers to the covalent attachment of the small ubiquitin-like modifier (SUMO), to protein substrates by the SUMO pathway.[24] SUMO is linked to its substrates by an iso-peptide bond between C-terminal carboxyl group of SUMO and ε-amino group of a lysine residue in the substrate. The SUMO E2 conjugating enzyme Ubc9, the second enzyme of a three-step catalytic cascade, covalently forms a thioester bond with SUMO, and selectively associates with and promotes the transfer of the SUMO to substrates.[25] SUMO E3 ligases, for example, the protein inhibitors of activated STATs (PIAS family proteins), form complexes with both the substrate and Ubc9, thereby facilitating the transfer of SUMO from E2 to the substrate. Sumoylation is a reversible process owing to the activity of sentrin-specific proteases (SENPs) that desumoylate SUMO protein substrates.[25,26] Because sumoylation has major functional consequences for its target substrates, there has been a great deal of interest in identifying novel SUMO substrates.

In this study, we have uncovered a novel sumoylation-dependent function for the ubiquitin ligase Smurf2 in TGFβ-induced EMT. Knockdown and gain-of-function analyses reveal that Smurf2 suppresses TGFβ-induced EMT in NMuMG mammary epithelial cells, a widely used cellular model system of EMT. In other experiments, we show that the SUMO E2 conjugating enzyme Ubc9 and the SUMO E3 ligase PIAS3 associate with Smurf2 and promote its sumoylation at

[1]Department of Biochemistry and Molecular Biology, Arnie Charbonneau Cancer Institute, Cumming School of Medicine, University of Calgary, Calgary, Canada
*Corresponding author: S Bonni, Department of Biochemistry and Molecular Biology, Arnie Charbonneau Cancer Institute, Cumming School of Medicine, University of Calgary, Room 377, Heritage Medical Research Building, 3330 Hospital Drive NW, Calgary, AB T2N 4N1, Canada. Tel: +1 403 210 8587; Fax: +1 403 283 8727; E-mail: sbonni@ucalgary.ca
[2]These authors contributed equally to this work.
Abbreviations: TGFβ, transforming growth factor-β; EMT, epithelial–mesenchymal transition; SUMO, small ubiquitin-like modifier; Smurf2, Smad (Sma and mad) ubiquitination regulatory factor-2; PIAS, protein inhibitor of activated STATs (signal transducers and activators of transcription); SENP, sentrin-specific protease; HECT, homology to E6 carboxy terminus domain; TβRI, TGFβ receptor 1; NEM, *N*-ethylmaleimide
Received 05.2.15; revised 09.10.15; accepted 19.10.15; Edited by N Chandel; published online 18.12.15

Lysines 26 and 369 in distinct cell types. The sumoylation of Smurf2 enhances its ability to trigger the degradation of the TGFβ receptor TβRI and thereby suppresses EMT. Taken together, our findings unveil an intimate new link between sumoylated Smurf2 and the regulation of EMT. Our studies point to an important regulatory role for sumoylation of Smurf2 in tissue morphogenesis and cancer progression.

Results

Smurf2 suppresses EMT. EMT is a fundamental process in development, with increasing evidence suggesting that it plays key roles in cancer cell invasion and metastasis.[27–29] TGFβ is a potent inducer of EMT in development and cancer,[3,30] and the canonical Smad signaling pathway contributes to the ability of TGFβ to promote EMT.[31–33] The E3 ubiquitin ligase Smurf2 associates with members of the Smad family of signaling proteins and thereby regulates TGFβ-mediated responses.[34,35] However, the role and regulation of Smurf2 in TGFβ-induced EMT has remained unexplored.

The nontransformed mammary NMuMG epithelial cells represent a well-established and suitable model to study EMT.[33,36,37] Growing evidence suggests that culturing epithelial cells in the context of an extracellular support system such as Matrigel provides a three-dimensional (3D) environment for cells resembling the stromal basement membrane under more 'physiological' conditions.[38–40] Accordingly, glandular-derived epithelial cells in a 3D matrix form acini with hollow centers similar to the morphology of these structures *in vivo*. Importantly, EMT disrupts the acinar morphology that manifests as filling of the hollow centers, outward invasiveness, and dysregulation of the abundance or localization of the epithelial marker protein E-cadherin.[38,40–43]

To determine the role of Smurf2 in EMT, we induced the knockdown of Smurf2 by RNA interference (RNAi) in NMuMG cells using transient transfection. Short hairpin RNAs (shRNAs) targeted against two distinct regions within Smurf2, alone or together, robustly downregulated exogenous Smurf2 in 293T cells and NMuMG mammary epithelial cells (Supplementary Figures S1A and B). Importantly, the two Smurf2 shRNAs, alone or together, also significantly reduced the abundance of endogenous Smurf2 in NMuMG cells (Figure 1a and Supplementary Figure S1C). We next determined the effect of Smurf2 knockdown on the ability of TGFβ to induce EMT in NMuMG cells. As expected, NMuMG cells seeded as single cells in 3D cultures formed organized hollow acini, and exposure to TGFβ led to filling and disorganization of these multicellular structures (Figure 1b).[40] In contrast, we found that Smurf2 knockdown by shRNA-1 and shRNA-2, separately or together, promoted filling of NMuMG cell-derived acini in the absence of TGFβ, and enhanced the ability of TGFβ to induce lumen filling and disorganization of NMuMG cell acini (Figure 1b and Supplementary Figure S1D). In immunocytochemical analyses, E-cadherin localized to intercellular junctions in control cells (Figure 1c and data not shown), and TGFβ reduced the abundance or mislocalized E-cadherin, consistent with EMT induction.[40] Smurf2 knockdown by shRNA-1 and shRNA-2, individually or together, further enhanced the ability of TGFβ to downregulate E-cadherin expression (Figure 1c and data not shown). These data suggest that endogenous Smurf2 inhibits TGFβ-induced EMT in epithelial cells.

In complementary experiments, expression of Smurf2 in NMuMG cells blocked the ability of TGFβ to disrupt the acinar morphology and downregulate E-cadherin in the 3D NMuMG cell-derived structures (Figures 1d–f). Importantly, expression of a rescue form of Smurf2 encoded by cDNA that is resistant to Smurf2 RNAi-1 ((Smurf2(r1)) or Smurf2 RNAi-2 (Smurf2(r2)), but not Smurf2 encoded by wild type cDNA, reversed the ability of Smurf2 knockdown by RNAi-1 or RNAi-2, respectively, to promote the filling of NMuMG-derived acini in the absence or presence of TGFβ (Figures 1g and h and Supplementary Figures S1E and F). Expression of Smurf2(r1) or Smurf2(r2) also reversed the ability of Smurf2 knockdown to enhance the ability of TGFβ to reduce or mislocalize E-cadherin in NMuMG-derived acini (Supplementary Figures S1G and H). Together, these data suggest that endogenous Smurf2 suppresses TGFβ-induced EMT in the nontransformed epithelial cells.

Smurf2 is a novel substrate of the SUMO pathway. The finding that Smurf2 suppresses TGFβ-induced EMT raised the question of how this novel function of Smurf2 is regulated in epithelial cells. Smurf2 has been suggested to be targeted by the ubiquitin–proteasome pathway.[44] However, we found no appreciable reduction in the abundance of Smurf2 in NMuMG cells undergoing TGFβ-induced EMT (Figure 1d). We, therefore, asked whether Smurf2 function in EMT might be regulated by sumoylation. Sumoylation of target proteins has profound consequences on the functions of target proteins. A cascade of three enzymes, a SUMO E1 activating enzyme, the SUMO E2 conjugating enzyme Ubc9, and a SUMO E3 ligase, promote the covalent attachment of the protein SUMO with target proteins. On the other hand, members of the SENP family of desumoylases remove SUMO from protein substrates.[25,26] The isopeptidase inhibitor *N*-ethylmaleimide (NEM) is included in lysis buffer to inhibit the SENP and preserve sumoylation of substrates.[45–47] Although free SUMO is $\sim$11 kDa in size, its conjugation adds an apparent molecular mass of $\geq$20 kDa to the molecular mass of the substrate in immunoblotting analyses.[25,46,48]

To determine whether Smurf2 might be sumoylated, we subjected NMuMG cell lysates prepared in sodium dodecyl sulfate (SDS)-containing lysis buffer in the absence or presence of NEM to immunoprecipitation with the Smurf2 antibody followed by immunoblotting with the SUMO and Smurf2 antibodies. Typically, only a small fraction of sumoylated protein substrate may be detected.[25] Thus, in addition to assessing endogenous Smurf2 sumoylation in NMuMG cells (Figure 2a, lanes 1 and 2), we included cells that express exogenous Smurf2 in these analyses (Figure 2a, lanes 4 and 5). We detected an NEM-sensitive 100 kDa SUMO-immunoreactive band in endogenous Smurf2 as well as exogenous Smurf2 immunoprecipitates (Figure 2a). In addition, higher-molecular-weight SUMO-immunoreactive protein bands appeared in the Smurf2 immunoprecipitates (Figure 2a, lane 5), suggesting that Smurf2 is sumoylated and

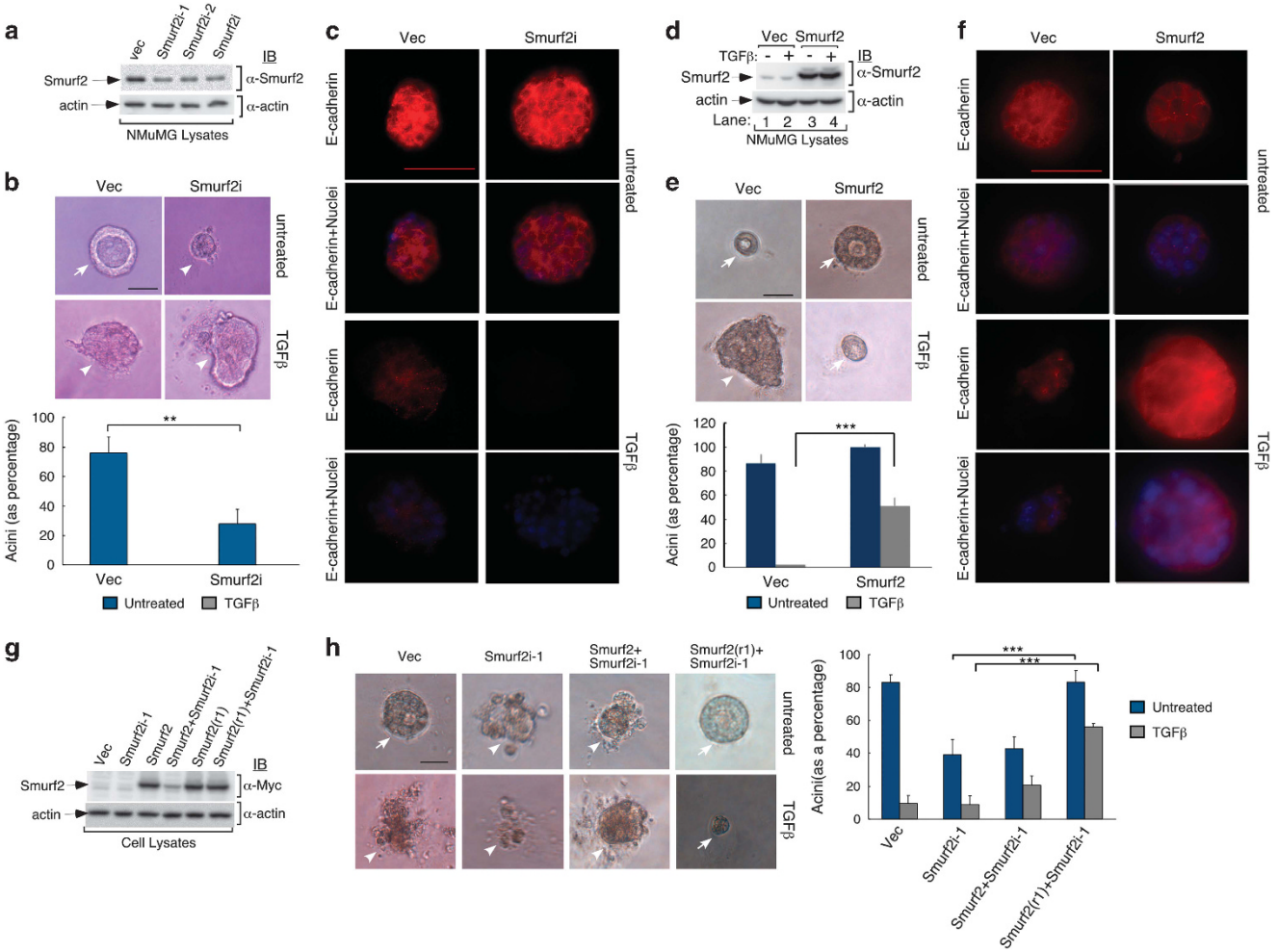

Figure 1 Smurf2 suppresses TGFβ-induced EMT in 3D NMuMG cultures. (**a**) Lysates of NMuMG cells transfected with an RNAi plasmid encoding short hairpin RNAs (shRNAs) targeting one of two unique sequences in Smurf2 (Smurf2i-1 or Smurf2i-2), added separately or as a pool (Smurf2i), or the corresponding control U6 RNAi plasmid, were immunoblotted with the Smurf2 or actin antibody, the latter serving as loading control. (**b**) Representative DIC images (top panel) and quantification of acini colony morphology (bottom panel, mean $\pm$ S.E.M., $n=4$) of 10-day-old 3D NMuMG cells transfected as in (**a**) and left untreated or incubated with 100 pM TGFβ. TGFβ reduced the proportion of acini with hollow centers (ANOVA, $P<0.001$). Smurf2 knockdown in NMuMG cells decreased the proportion of acini with hollow structures even in the absence of TGFβ as compared with cells expressing vector control (ANOVA, $^{**}P<0.01$). (**c**) The 3D NMuMG cultures as in (**b**) were subjected to immunocytochemistry using E-cadherin (red) antibody and Hoechst 33258 (blue). (**d**) Lysates of vector control or Smurf2-transfected NMuMG cells left untreated or incubated with TGFβ were immunoblotted with the Smurf2 or actin antibody, the latter representing a loading control. (**e**) Representative DIC images (top panel) and quantification of acini colony morphology (bottom panel, mean $\pm$ S.E.M., $n=4$) of 10-day-old 3D NMuMG cells transfected and treated as in (**b**). Wild-type Smurf2 significantly suppressed the ability of TGFβ to reduce the proportion of hollow acini ($^{***}P<0.001$). (**f**) The 3D NMuMG cultures as in (**e**) were subjected to immunocytochemistry using E-cadherin (red) antibody and Hoechst 33258 (blue). (**g**) Lysates of NMuMG cells transfected with RNAi plasmid encoding Smurf2 shRNA-1 or the control U6 RNAi plasmid together with an expression plasmid encoding an RNAi-resistant MYC-tagged Smurf2 (Smurf2(r1)) or Smurf2 encoded by WT cDNA, or the corresponding vector control, were immunoblotted with the MYC or actin antibody. (**h**) Representative DIC images (left panel) and quantification of acini colony morphology (right panel, mean $\pm$ S.E.M., $n=3$) of 10-day-old 3D NMuMG cells transfected with the RNAi plasmid encoding Smurf2 shRNA-1 (Smurf2i-1), together with an expression plasmid encoding an RNAi-resistant MYC-tagged Smurf2 (Smurf2(r1)) or a Smurf2 encoded by WT cDNA or the corresponding plasmid control, or with the control plasmids, and treated as in (**b**). Expression of Smurf2(r1), but not WT Smurf2, reversed Smurf2i-1-induced NMuMG cell-derived acini filling in the absence or presence of TGFβ (ANOVA, $^{***}P<0.001$). Scale bar = 50 μm (**b**, **c**, **e**, **f**, and **h**). Arrows and arrowheads indicate intact and disrupted acini, respectively

poly-sumoylated in NMuMG cells. Notably, unmodified Smurf2 was detected as an 80-kDa protein (Figure 2a). Corroborating these results, immunoblotting analyses of Smurf2 immunoprecipitates or lysates of NMuMG cells with the Smurf2 antibody revealed NEM-sensitive higher-molecular-weight endogenous as well as exogenous Smurf2-immunoreactive bands (Figure 2a, middle panel, and Figure 2b). In other experiments, immunoprecipitation of endogenous Smurf2 followed by immunoblotting with the SUMO antibody or Smurf2 antibody revealed that endogenous Smurf2 is sumoylated in NMuMG cells (Figure 2c). To gain further evidence for Smurf2 sumoylation, we carried out *in vivo* sumoylation assays in 293T cells that are widely used in sumoylation analyses.[45] We expressed MYC-tagged Smurf2, HA-tagged SUMO, or both proteins together in 293T cells and subjected their lysates to immunoprecipitation with the MYC antibody followed by immunoblotting with the HA or MYC antibody. Expression of SUMO with Smurf2 led to the appearance of a 100-kDa as well as poly-sumoylated Smurf2 in an NEM-sensitive manner (Figure 2d). Collectively, these

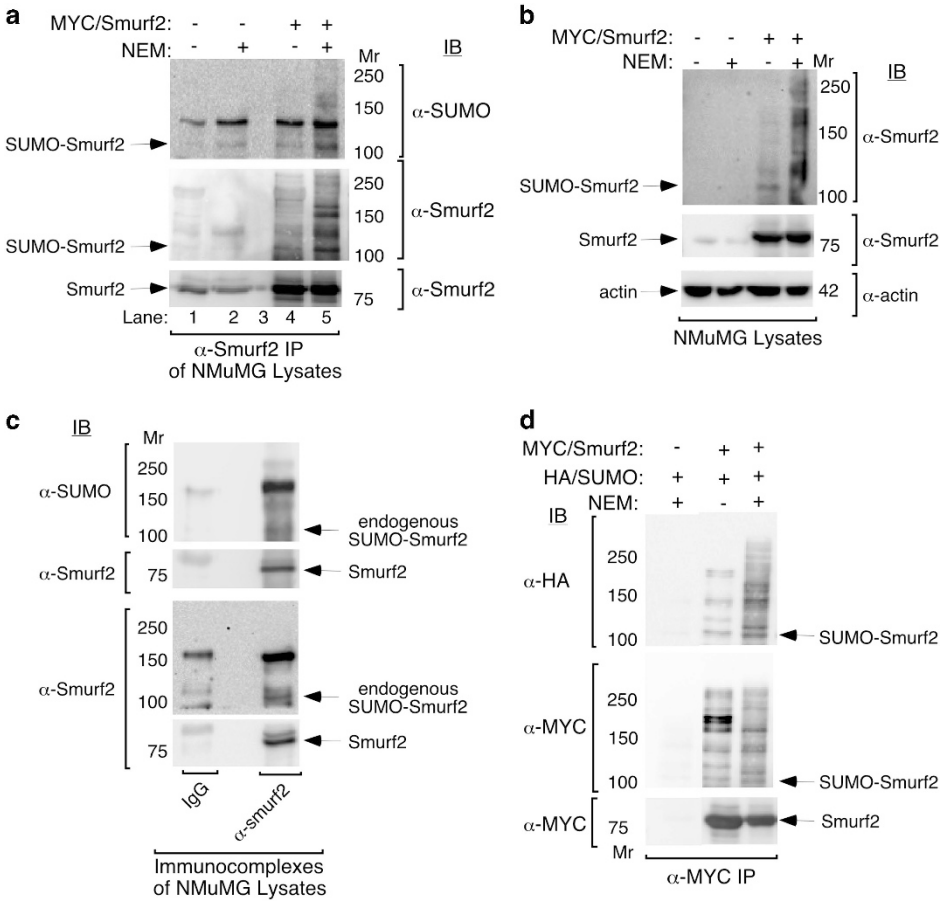

Figure 2 Smurf2 is a novel substrate of the SUMO pathway. (**a**) NMuMG cells stably expressing Smurf2 or transfected with the vector control were lysed in the absence or presence of the general isopeptidase inhibitor NEM and immunoprecipitated with Smurf2 antibody (Smurf2 IP) followed by immunoblotting (IB) with the SUMO or Smurf2 antibody to visualize sumoylated-Smurf2 protein species (upper and middle panels) and unmodified Smurf2 (lower panel) in the Smurf2 immunocomplexes. The arrow in the upper blot indicates an NEM-sensitive SUMO-immunoreactive protein species in Smurf2 immunocomplexes of lysates of NMuMG cells expressing endogenous Smurf2 (lanes 1 and 2) or exogenous Smurf2 (lanes 4 and 5) running at molecular mass of ~100 kDa. The arrow in the middle blot points to an NEM-sensitive Smurf2-immunoreactive protein band running at an approximate molecular mass of 100 kDa. (**b**) The expression of endogenous and expressed Smurf2 in lysates of NMuMG cells as described in (**a**) was confirmed by immunoblotting with the Smurf2 antibody. Blotting for actin in cell lysates was used as a loading control. Upper blot shows an NEM-sensitive Smurf2-immunoreactive protein species at ~100 kDa clearly seen in cells overexpressing Smurf2 (arrow). (**c**) NEM-treated lysates of NMuMG cells were subjected to Smurf2 or IgG immunoprecipitation followed by SUMO immunoblotting. Immunoprecipitation of Smurf2 was confirmed by immunoblotting using the Smurf2 antibody. (**d**) Lysates of 293T cells expressing HA-tagged SUMO alone or together with MYC-tagged Smurf2 and prepared in the absence or presence of NEM were subjected to immunoprecipitation with the MYC antibody followed by immunoblotting (IB) with the HA antibody to visualize sumoylated protein species (upper panel). The blots were probed with MYC antibody to ascertain the abundance of unmodified Smurf2 (lower panel) and modified Smurf2 in the MYC immunoprecipitation (middle panel). Arrows in the upper and middle blots indicate co-migrating NEM-sensitive sumoylated Smurf2 species. M_r indicates markers' molecular size

data suggest that Smurf2 is modified by the SUMO pathway in cells.

The SUMO E2 enzyme Ubc9 promotes sumoylation by association with its substrates.[25] In coimmunoprecipitation analyses, we found that Ubc9 forms a complex with Smurf2 in cells (Figure 3a). We next determined the effect of expression of wild-type Ubc9 or a SUMO-conjugating inactive Ubc9 mutant, in which the catalytic Cysteine 93 is replaced with serine (CS),[49,50] on exogenous Smurf2 sumoylation in 293T cells. Expression of wild-type Ubc9, but not Ubc9 (CS), enhanced the sumoylation of exogenous Smurf2 in 293T cells (Figures 3b and c). Expression of Ubc9 also led to robust sumoylation of endogenous Smurf2 in NMuMG cells (Supplementary Figure S2A). Together, these data demonstrate that Ubc9 associates with and promotes the sumoylation of Smurf2.

We next determined the role of SUMO E3 ligases in Smurf2 sumoylation. PIAS represent the largest family of SUMO E3 ligases.[50,51] We measured the effect of expression of the four PIAS family members PIAS1, PIAS2, PIAS3, or PIAS4 on Smurf2 sumoylation in 293T cells.[25,45,51] Among the PIAS proteins, PIAS3 enhanced Smurf2 sumoylation (Figures 3d and e and data not shown). In reciprocal coimmunoprecipitation studies, we found that Smurf2 and PIAS3 form a complex in cells (Figure 3f). Importantly, we found that PIAS3 enhanced sumoylation of endogenous Smurf2 in NMuMG cells (Supplementary Figure S2B).

Sumoylation is a dynamic and reversible process due to the action of the SUMO cleaving SENP family of isopeptidases.[25,52] Employing *in vivo* sumoylation assays, we observed that expression of SENP1 or SENP2 but not SENP3 led to complete loss of the 100 kDa and

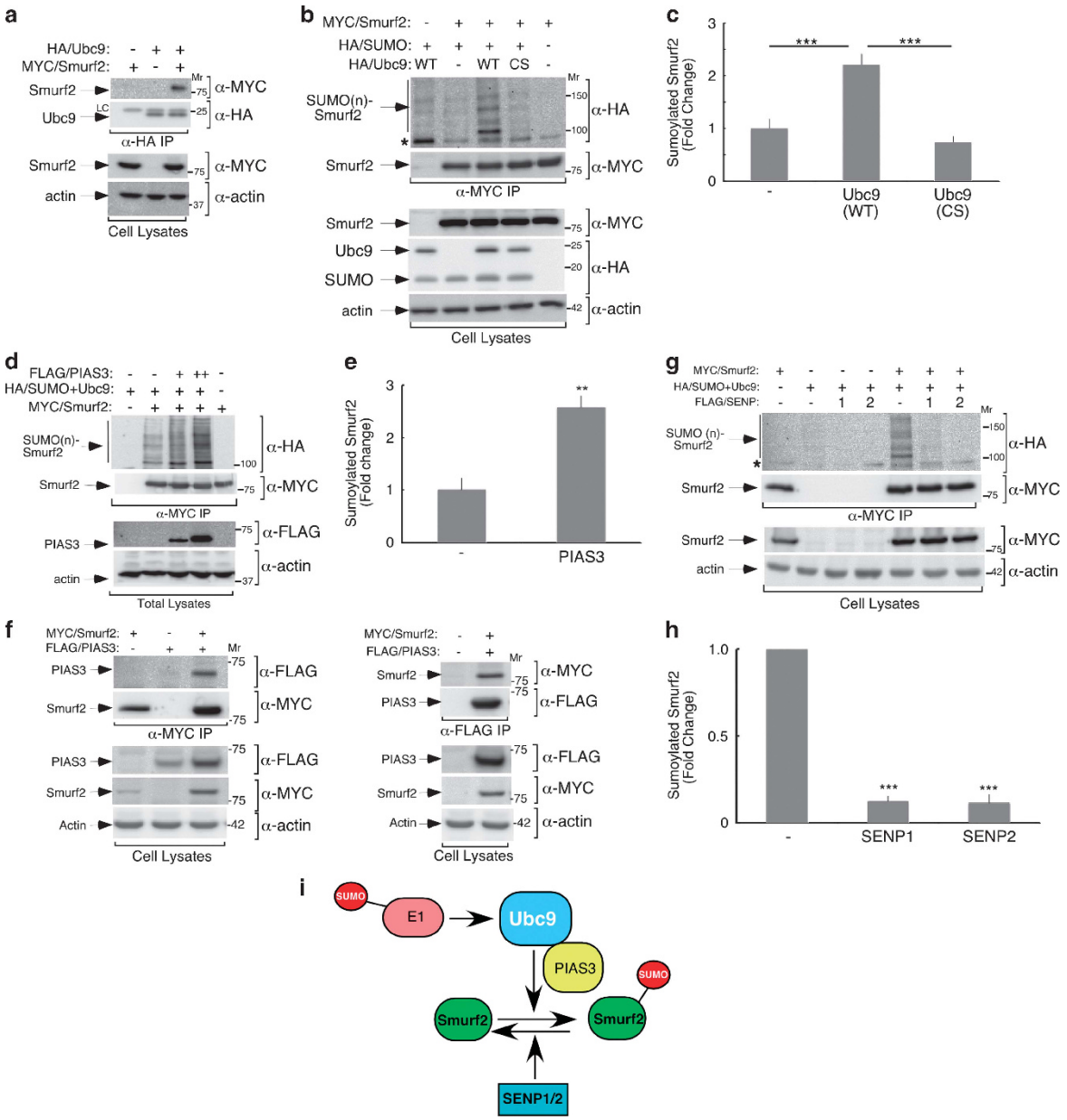

Figure 3 The SUMO E2 enzyme Ubc9 and the SUMO E3 ligase PIAS3 promote and the SUMO isopeptidases SENP1/2 inhibit Smurf2 sumoylation. (**a**) Lysates of 293T cells expressing MYC-tagged Smurf2 and HA-tagged Ubc9 alone or together were subjected to Ubc9 immunoprecipitation (HA IP) followed by Smurf2 (MYC) and Ubc9 (HA) immunoblotting. Smurf2 protein abundance in the lysates was confirmed by Smurf2 immunoblotting (MYC IB). Immunoblotting for actin in lysates was used as loading control. LC, light chain. (**b**) NEM-treated lysates of 293T cells expressing MYC-tagged Smurf2, HA-tagged SUMO, WT Ubc9, or an E2 SUMO conjugating inactive Ubc9 in which Cysteine 93 is converted to serine (CS) were subjected to *in vivo* sumoylation assay as described in Figure 2d. Expression of MYC/Smurf2, mono/di HA/SUMO, or HA/Ubc9 was confirmed by immunoblotting with the MYC and HA antibodies. Actin immunoblotting was used as a loading control. Note SUMO is conjugated to protein substrates and can be detected as higher molecular species compared with unmodified substrate. Ubc9 promotes the sumoylation of Smurf2. *Indicates a nonspecific band. (**c**) The bar graph shows the proportion of sumoylated Smurf2 relative to unmodified Smurf2 in the absence and presence of WT or CS Ubc9 as expressed relative to proportion of Smurf2 sumoylation in the absence of Ubc9 (mean ± S.E.M., $n=4$). (**d**) Lysates of 293T cells expressing MYC-tagged Smurf2 alone or together with Ubc9 and SUMO, alone or together with a low (+) and high (++) concentrations of the SUMO E3 ligase PIAS3 (FLAG-PIAS3), were subjected to Smurf2 sumoylation assay as described in Figure 2d (upper panel). Expression of FLAG-tagged PIAS3 was confirmed in cell lysates. Actin was used as a loading control. (**e**) The bar graph depicts the proportion of SUMO-conjugated Smurf2 in the absence or presence of PIAS3 expressed relative to the proportion of sumoylated Smurf2 in the absence of PIAS3 (mean ± S.E.M., $n=4$). (**f**) Lysates of cells expressing FLAG-tagged PIAS3 and MYC-tagged Smurf2, alone or together, were subjected to immunoprecipitation for Smurf2 (MYC IP) or PIAS3 (FLAG IP) followed by immunoblotting for PIAS3 (FLAG IB, first panel) or Smurf2 (MYC IB, sixth panel), respectively. Immunoprecipitation of Smurf2 (MYC IB, second panel) and PIAS3 (FLAG IB, seventh) was confirmed. Expression of Smurf2 (MYC IB) and PIAS3 (FLAG IB) in lysates was assessed by immunoblotting, with actin used as loading control. (**g**) Lysates of 293T cells expressing Ubc9 and SUMO alone or together with different combinations of MYC-tagged Smurf2, FLAG-tagged SENP1, or SENP2 were subjected to a Smurf2 sumoylation assay (upper panel). Expression of MYC-tagged Smurf2 was confirmed in cell lysates as described in (**a**). *Indicates a nonspecific band. (**h**) The bar graph shows the proportion of sumoylated Smurf2 normalized to unmodified Smurf2 and expressed relative to sumoylated Smurf2 in the absence of SENP1 or SENP2 coexpression (mean ± S.E.M., $n=4$). (**i**) The SUMO E2 conjugating enzyme Ubc9 acts together with the SUMO E3 ligase PIAS3 to associate and promote the sumoylation of Smurf2 in cells. Significant difference $^{**}P<0.01$ and $^{***}P<0.001$ (ANOVA or *t*-test)

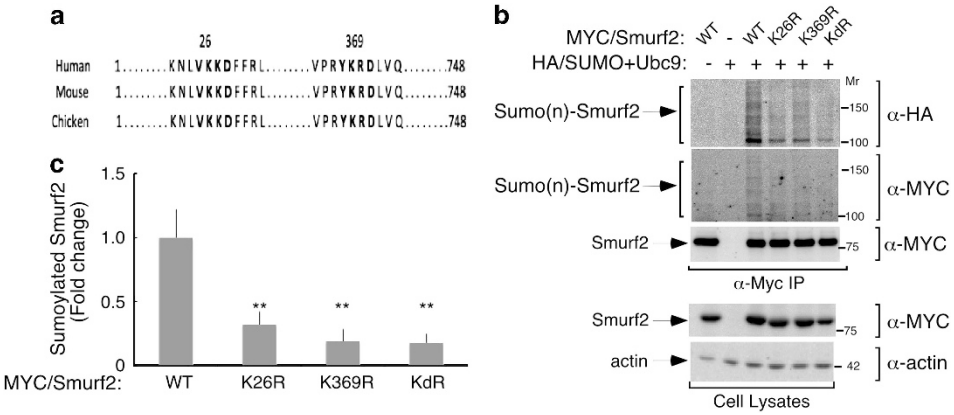

Figure 4 Lysines 26 and 369 are major sites of sumoylation in Smurf2. (**a**) Sequence alignment of the human, mouse, and chicken Smurf2 protein showing the regions that contain the two conserved sumoylation consensus motifs. (**b**) Smurf2 sumoylation assays in 293T cells expressing HA-tagged SUMO and Ubc9, alone or together with wild type Smurf2 (WT), or one of three Smurf2 SUMO mutants in which either Lysines 26 and 369 were converted individually or together to arginine (K26R), (K369R), or (KdR). Expression of Smurf2 was confirmed by immunoblotting lysates with the MYC antibody. Immunoblotting for actin was used as a loading control. Results shown in (**b**) are from a representative experiment that was repeated four times. (**c**) The bar graph shows the proportion of sumoylated Smurf2 normalized to the unmodified Smurf2 and expressed relative to that of WT Smurf2 control (mean ± S.E.M., $n=4$). Significant difference $^{**}P<0.01$ (ANOVA)

higher-molecular-mass SUMO-immunoreactive bands in the Smurf2 immunoprecipitates (Figures 3g and h and data not shown), suggesting that SENP1 and SENP2 catalyze the desumoylation of Smurf2 in cells. Collectively, our results suggest that the SUMO E2 enzyme Ubc9 and the SUMO E3 ligase PIAS3 promote whereas the SUMO isopeptidases SENP1/2 inhibit the sumoylation of Smurf2 (see model in Figure 3i).

We next mapped the lysine residues within Smurf2 that are covalently linked to SUMO. SUMO is conjugated to substrates at lysine residue residing in a consensus SUMO motif, ψKXD/E, where ψ is a large hydrophobic residue, K is a lysine residue, X denotes any amino acid, and E/D refer to glutamic acid or aspartic acid, respectively. Using the SUMOplot software (Abgent, San Diego, CA, USA) and SUMO sp2.0 (Guangzhou, China), we identified two specific lysine residues, K26 and K369, as putative consensus sites of sumoylation motifs that are conserved in human, mouse, and chicken Smurf2 (Figure 4a). To test whether one or both lysine residues corresponding to residues 26 and 369 of human Smurf2 are sumoylated, we expressed in 293T cells human Smurf2 with either Lysine 26 (K26R) or 369 (K369R) or both residues (KdR) mutated to arginine. Mutation of Lysines 26 and 369, alone or together, reduced the level of Smurf2 sumoylation, suggesting that these lysines are major SUMO acceptor sites in Smurf2 (Figures 4b and c). We also characterized the sumoylation sites in Smurf2 that was expressed as part of a *Renilla* fusion protein (Rluc-Smurf2) in 293T and NMuMG cells. Unmodified Rluc-Smurf2 had an apparent molecular mass of ~125 kDa, and accordingly sumoylated Rluc-smurf2 was detected with an approximate molecular mass of 145 kDa in 293T and NMuMG cells (Supplementary Figures S3A and B). Mutation of Lysines 26 and 369 abrogated sumoylated Rluc-Smurf2 in these cells (Supplementary Figures S3A and B). Taken together, our results suggest that Lysines 26 and 369 are major SUMO acceptor sites in Smurf2 in different cell types.

Sumoylated Smurf2 suppresses TGFβ-induced EMT. Next, we determined the role of sumoylation of Smurf2 in its ability to suppress EMT.

We compared the effect of wild-type Smurf2 (Smurf2WT) or a SUMO loss-of-function Smurf2 mutant in which Lysines 26 and 369 were replaced with arginine (Smurf2KdR) on TGFβ-induced disruption of morphogenesis of acini in 3D NMuMG cultures in the absence or presence of TGFβ (100 pM) for 10 days. Expression of Smurf2WT suppressed TGFβ-induced lumen filling and disorganization of NMuMG acini (Figures 1e and 5b). In contrast, expression of Smurf2KdR failed to suppress TGFβ-induced lumen filling and disorganization of NMuMG acini (Figure 5b). Rather, expression of Smurf2KdR enhanced lumen filling of NMuMG acini, thus phenocopying the effect of Smurf2 knockdown (Figures 1b and h and 5b and Supplementary Figures S1D and F). Accordingly, immunocytochemical analyses using the E-cadherin antibody showed that Smurf2WT blocked whereas Smurf2KdR promoted the ability of TGFβ to downregulate and disrupt the localization of E-cadherin (Figure 5c). These data suggest that sumoylation is critical for the ability of Smurf2 to suppress TGFβ-induced EMT in 3D NMuMG-derived acini structures.

We next assessed the role of the TGFβ–Smad pathway in the ability of sumoylated Smurf2 to suppress EMT. TGFβ binds and assembles type I and II Ser/Thr kinase cell surface receptors into an active heteromeric complex, whereby the activated type I receptor kinase stimulates downstream signaling events and consequent responses including EMT.[53,54] We compared the effect of blockade of the type I kinase receptor by the small molecule inhibitor, SB431542, on the ability of Smurf2 knockdown or the SUMO loss of function Smurf2 mutant (Smurf2KdR) to promote acini filling and disorganization (Figures 6a and b and Supplementary Figures S4A and B). As expected, incubation of the vector-transfected NMuMG cell-derived 3D multicellular organoids with the TGFβ receptor kinase inhibitor promoted acini formation and maintenance, and enhanced E-cadherin

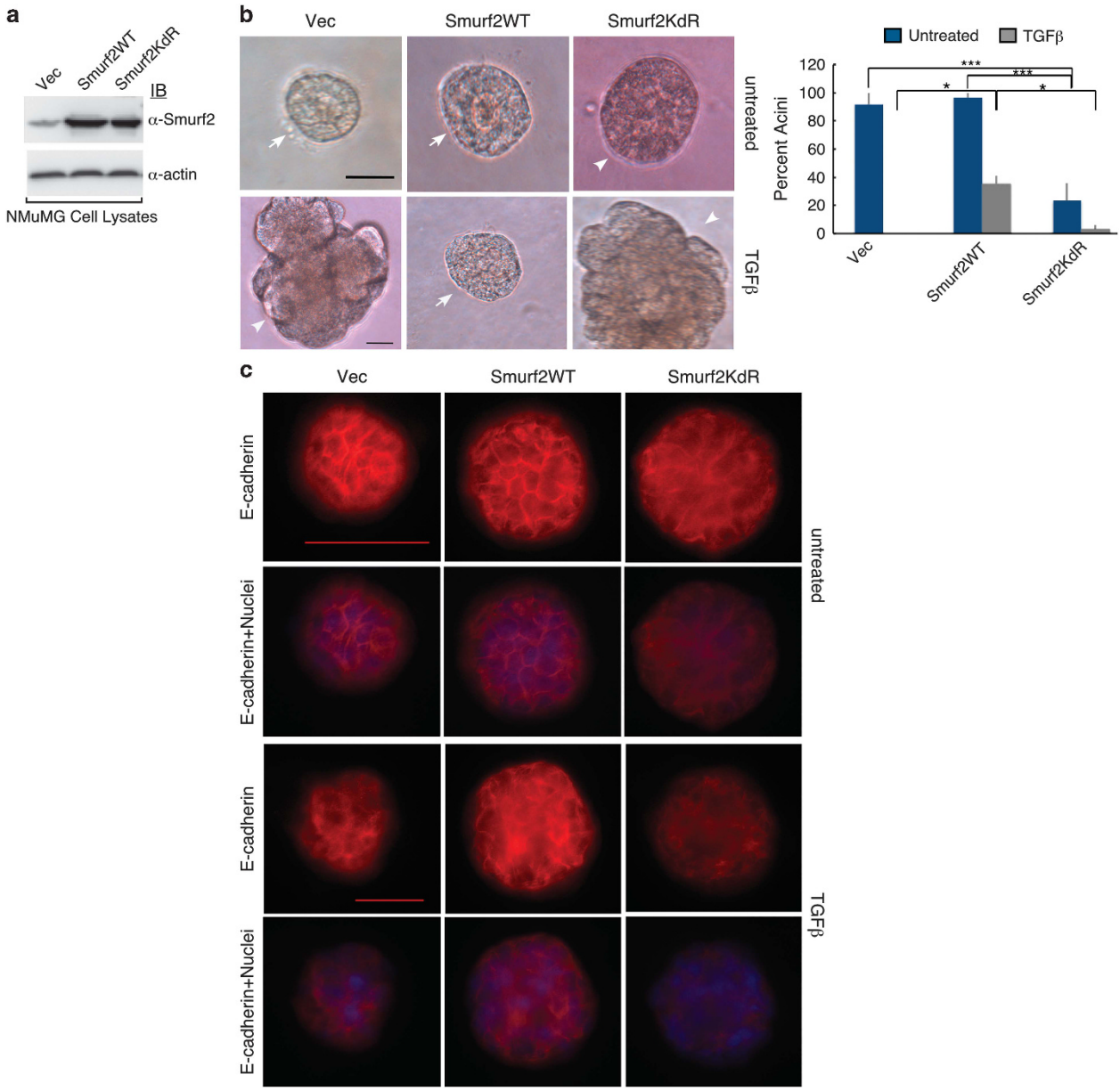

Figure 5 Smurf2 acts in a sumoylation-dependent manner to regulate epithelial morphogenesis. (**a**) Lysates of NMuMG cells expressing WT Smurf2 or the SUMO loss-of-function Smurf2 in which Lysines 26 and 369 were converted into arginine (KdR) or cells transfected with the vector control were immunoblotted with the Smurf2 antibody. (**b**) Representative DIC images of untreated or 100 pM TGFβ-incubated 10-day-old 3D multicellular structures (including acini) of NMuMG cells expressing WT or SUMO loss-of-function Smurf2 or transfected with the vector control as described in (**a**). The bar graph depicts the proportion of NMuMG-derived colonies showing hollow acini as an indicator of colony morphology (mean $\pm$ S.E.M., $n=3$). Smurf2 significantly suppressed the ability of TGFβ to reduce the proportion of hollow acini (ANOVA, $^{*}P<0.05$). In contrast, the SUMO loss-of-function Smurf2KdR mutant decreased the proportion of acini with hollow centers in the presence or absence of TGFβ (ANOVA, $^{***}P<0.001$). (**c**) The 3D NMuMG cultures as in (**b**) were analyzed for the adherens junction protein E-cadherin abundance and localization. Cells were identified by nuclear staining as described in Figure 1c.Scale bar = 50 μm (**b** and **c**). Arrows and arrowheads indicate intact and disrupted acini, respectively

abundance in the presence or absence of TGFβ (Figures 6a and b and Supplementary Figures S4A and B).[40] Remarkably, the Smurf2 knockdown- or Smurf2KdR-induced acini filling and disorganization and loss or mislocalization of E-cadherin were reversed by blockade of the TGFβ Ser/Thr kinase receptors in the presence or absence of TGFβ (Figures 6a and b and Supplementary Figures S4A and B), suggesting that TGFβ receptor-mediated signaling is a target for sumoylated Smurf2 to suppress EMT.

The signaling proteins Smad2 and Smad3 are major downstream mediators of TGFβ-induced responses including EMT.[55] Accordingly, knockdown of Smad2 or Smad3 suppressed, whereas expression of Smad2 or Smad3 promoted, the ability of TGFβ to induce EMT in the 3D NMuMG cell-derived acini (Supplementary Figures S5A–D). Importantly, we found that knockdown of Smad3 drastically suppressed the ability of Smurf2 knockdown or Smurf2KdR expression to induce acini filling and disorganization of NMuMG organoids in

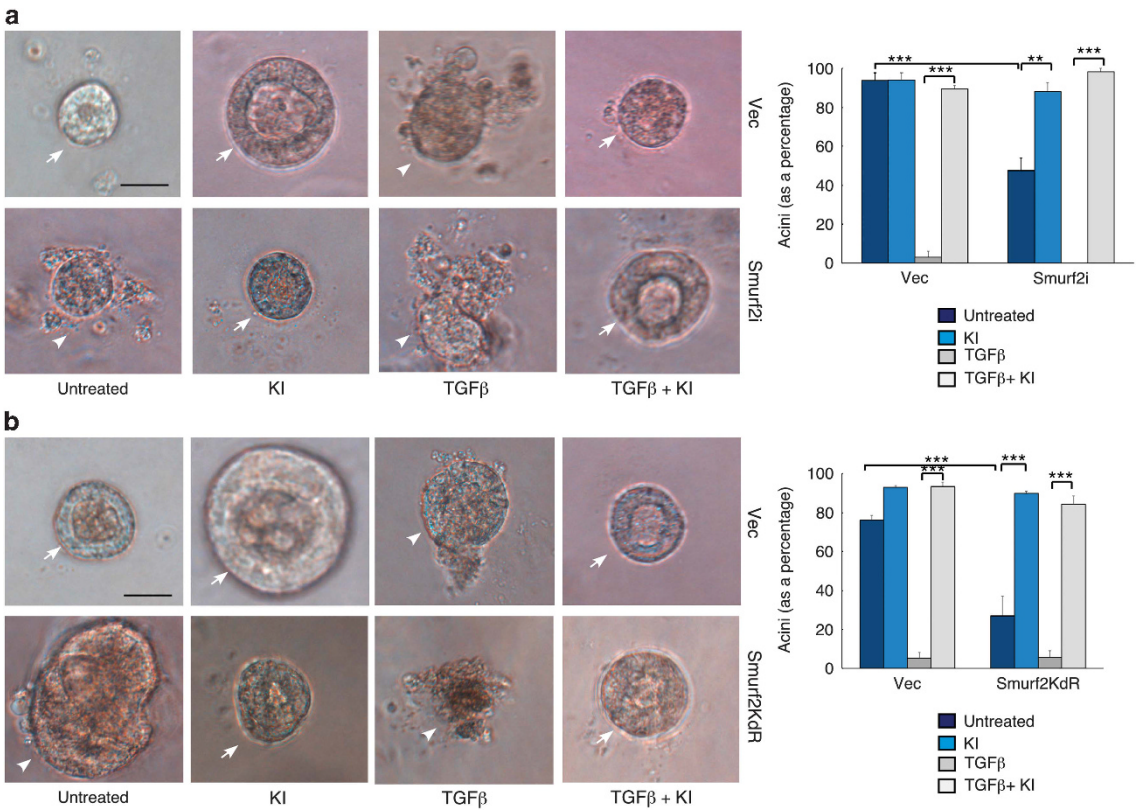

Figure 6 Sumoylated Smurf2 inhibits epithelial morphogenesis via regulation of TGFβ receptors. (**a**) Representative DIC images of 10-day-old 3D multicellular structures (including acini) of NMuMG cells transfected with the Smurf2 RNAi plasmid or control U6 RNAi plasmid that were left untreated or incubated with TGFβ type I receptor kinase inhibitor SB431542 (KI) (10 μM) and TGFβ (100 pM), alone or together. The bar graph depicts the proportion of NMuMG-derived colonies showing hollow acini as an indicator of colony morphology (mean $\pm$ S.E.M., $n=4$). The TGFβ receptor inhibitor (KI) significantly suppressed the ability of TGFβ to reduce the proportion of hollow acini in control cells (ANOVA, $^{***}P<0.001$). In addition, KI blocked the ability of Smurf2 knockdown to reduce the proportion of acini with hollow centers in the absence or presence of TGFβ (ANOVA, $^{**}P<0.01$, $^{***}P<0.001$). (**b**) Representative DIC images of 10-day-old 3D multicellular structures (including acini) of NMuMG cells transfected with an empty mammalian vector or an expression plasmid encoding Smurf2KdR and treated as described in (**a**). The bar graph depicts the proportion of NMuMG-derived colonies showing hollow acini as an indicator of colony morphology (mean $\pm$ S.E.M., $n=4$). The TGFβ receptor inhibitor (KI) significantly suppressed the ability of TGFβ to reduce the proportion of hollow acini in control cells (ANOVA, $^{***}P<0.001$) and the ability of Smurf2KdR to reduce the proportion of acini with hollow centers in the presence or absence of TGFβ (ANOVA, $^{***}P<0.001$). Scale bar = 50 μm (**a** and **b**). Arrows and arrowheads indicate intact and disrupted acini, respectively

the absence or presence of TGFβ (Figures 7a and b). In immunofluorescence analyses, Smad3 knockdown also suppressed the downregulation of E-cadherin and its mislocalization upon Smurf2 knockdown or expression of Smurf2KdR (Supplementary Figures S5E and F). Taken together, these data suggest that sumoylated Smurf2 suppresses EMT via regulation of the TGFβ-Smad pathway.

Smurf2 promotes the ubiquitin-mediated degradation of the TGFβ type I receptor.[23,35] To gain insight into the mechanisms by which sumoylated Smurf2 suppresses TGFβ-induced EMT, we compared the ability of Smurf2WT and Smurf2KdR to reduce the abundance of the TGFβ type I receptor (TβRI). As expected, Smurf2WT substantially reduced the abundance of TβRI in cells (Figure 8a). In contrast, expression of Smurf2KdR failed to effectively reduce the levels of TβRI (Figure 8a). The inability of Smurf2KdR to efficiently reduce the levels of the TβRI was not due to lack of association, as coimmunoprecipitation analyses demonstrated that Smurf2KdR interacts, similar to Smurf2WT, with activated TβRI (TβRI (TD); Figure 8b), suggesting that sumoylation promotes the ability of Smurf2 to induce the degradation of TβRI. Smad7 and Smurf2 associate in a bipartite manner whereby Smad7's N-terminal domain (NTD) and PPXY motif interact with Smurf2's HECT and WW domains, respectively. In particular, the NTD–HECT association promotes the autoubiquitination activity of Smurf2 by recruiting E2s to Smurf2.[35,44,56] In control analyses, the KdR mutation had little or no effect on the association of Smurf2 with Smad7 or on Smad7-induced downregulation of Smurf2 (Figures 8c and d). Notably, Lysine 369 is located N-terminal to the HECT domain (Figure 8e). Together, these observations suggest that the KdR mutation does not have nonspecific effects on the interaction of Smurf2 with cognate E2 or on Smurf2 autoregulation. The C2 domain of Smurf2 associates with the HECT domain to inhibit Smurf2 autoregulation.[44] Lysine 26 resides in the N-terminal region of the C2 domain (Figure 8e). In additional control analyses, conversion of Lysine 26 or 369 to arginine failed to reduce the interaction of the C2 and HECT domains (Figure 8f), suggesting that the KdR mutation does not have nonspecific effects on intramolecular interaction of Smurf2 (Figure 8f). The C2 domain regulates Smurf2 localization in cells.[56,57] In control immunofluorescence analyses, Smurf2WT and Smurf2KdR showed similar subcellular localization in NMuMG cells (Figure 8g).

Taken together, our data support the idea that sumoylation of Smurf2 enhances its ability to promote TGFβ receptor degradation and thereby suppresses EMT.

Collectively, we have identified a novel PIAS3–Smurf2 sumoylation link that suppresses TGFβ-induced EMT (see model in Figure 8h).

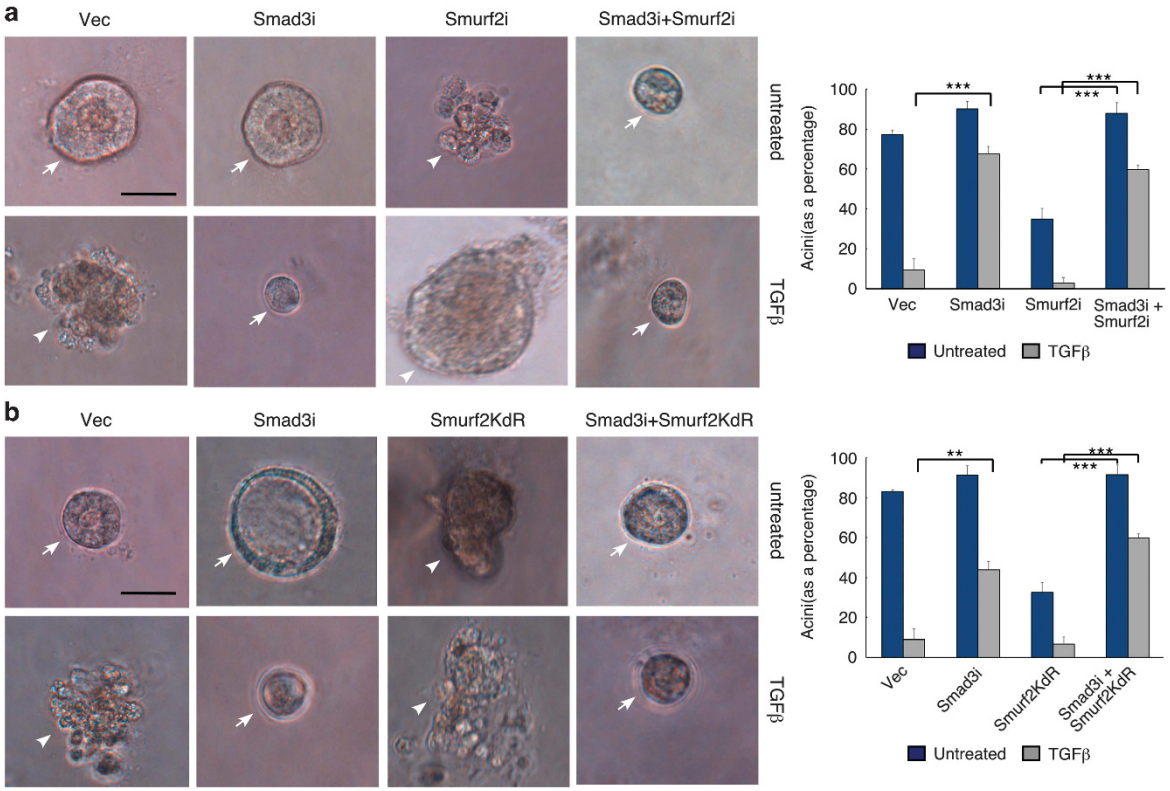

Figure 7 Sumoylated Smurf2 suppresses epithelial morphogenesis via regulation of Smad3 signaling. (**a**) Representative DIC images of untreated or 100 pM TGFβ-incubated 10-day-old 3D multicellular structures (including acini) of NMuMG cells transfected with different combinations of the Smurf2 and Smad3 RNAi plasmids or the corresponding control U6 RNAi plasmid. The bar graph depicts the proportion of NMuMG-derived colonies showing hollow acini as an indicator of colony morphology (mean $\pm$ S.E.M., $n=4$). Knockdown of endogenous Smad3 significantly suppressed the ability of TGFβ to reduce the proportion of hollow acini in control cells (ANOVA, $^{***}P<0.001$). In addition, Smad3 knockdown blocked the ability of Smurf2 knockdown to reduce the proportion of acini with hollow centers in the presence or absence of TGFβ (ANOVA, $^{***}P<0.001$). (**b**) Representative DIC images of untreated and 100 pM TGFβ-incubated 10-day-old 3D multicellular structures (including acini) of NMuMG cells co-transfected with the Smad3 RNAi plasmid, an expression plasmid encoding Smurf2KdR, or their control vectors. The bar graph depicts the proportion of NMuMG-derived colonies showing hollow acini as an indicator of colony morphology (mean $\pm$ S.E.M., $n=4$). Smad3 knockdown significantly suppressed the ability of TGFβ to reduce the proportion of hollow acini in control cells (ANOVA, $^{**}P<0.01$), and also blocked the ability of Smurf2KdR to reduce the proportion of acini with hollow centers in the presence or absence of TGFβ (ANOVA, $^{***}P<0.001$). Scale bar = 50 μm (**a** and **b**). Arrows and arrowheads indicate intact and disrupted acini, respectively

Figure 8 Sumoylation is required for Smurf2-induced degradation of TβRI. (**a**) Lysates of 293T cells transfected with expression plasmids encoding C-terminal HA-tagged TGFβ type I receptor (TβRI), C-terminal HIS-tagged TGFβ type II receptor (TβRII), and Smad7, together with a vector control or a plasmid encoding MYC-tagged WT Smurf2 (Smurf2WT) or Smurf2KdR, were subjected to TβRI (α-HA), TβRII (α-TβRII), Smurf2 (α-MYC), and actin immunoblotting, the latter serving as the loading control. Left, representative immunoblot from an experiment that was repeated five independent times. Right, mean ($\pm$S.E.M., $n=5$) of actin/normalized TβRI levels. Expression of Smurf2WT reduced the abundance of TβRI, whereas expression of Smurf2KdR failed to efficiently reduce the level of TβRI (ANOVA, $^{*}P<0.05$, $^{***}P<0.001$). (**b**) Lysates of 293T cells transfected with an expression plasmid encoding an HA-tagged constitutively active TβRI in which Threonine 204 is converted to Aspartate (TβRI (TD)) or the control vector together with MYC-tagged Smurf2WT or Smurf2KdR expressing, or their control vector were subjected to Smurf2 immunoprecipitation (α-MYC IP) followed by TβRI (α-HA) and Smurf2 (α-MYC) immunoblotting. Expression of TβRI(TD) was confirmed by immunoblotting. (**c**) Lysates of cells transfected with a plasmid encoding MYC-tagged Smurf2WT or Smurf2KdR, alone or together with HA-tagged Smad7, or the empty vector were subjected to Smurf2 (α-MYC), Smad7 (α-HA), and actin immunoblotting, the latter serving as the loading control. Left, representative immunoblot from an experiment that was repeated four independent times. Right, mean ($\pm$S.E.M., $n=4$) of actin/normalized Smurf2 levels. Reduction of Smurf2WT is comparable to the reduction in the level of Smurf2KdR upon coexpression of Smad7 (ANOVA, $^{***}P<0.001$). (**d**) Lysates of cells transfected as in (**c**) were subjected to Smad7 immunoprecipitation (α-HA IP) followed by Smurf2 (α-MYC) and Smad7 (α-HA) immunoblotting. Expression of Smad7 was confirmed by immunoblotting. (**e**, upper) A schematic of Smurf2 showing the C2 (yellow), WW (mauve), and HECT (green) domains, and relative location of Lysines 26 and 369 with respect to the C2 and HECT domains. Middle and lower schematics depict the C2-WW-containing (Smurf2C2) and WW-HECT-containing (Smurf2HECT) Smurf2 deletion proteins expressed in experiments shown in (**f**). (**f**) Lysine 26 or Lysine 369 mutation to arginine does not affect the C2-HECT association. Affinity purified FLAG-tagged Smurf2C2 (WT) or Smurf2C2(K26R) expressed in 293T cells, with the vector transfected cells used as control, using anti-FLAG antibody immunoprecipitation followed by FLAG peptide elution with each sample divided into three equal aliquots and incubated with lysates of cells transfected with the control vector, MYC-tagged Smurf2HECT(WT), or Smurf2HECT (K369R) expression plasmid, subjected to anti-MYC immunoprecipitation (α-MYC IP) followed by FLAG and MYC immunoblotting. Expression of FLAG-tagged proteins was confirmed in cell lysates. HC denotes heavy chain of the MYC antibody. (**g**) Representative images of TGFβ-treated NMuMG cells expressing Smurf2WT or Smurf2KdR and subjected to immunocytochemistry using the anti-Smurf2 antibody (red). Nuclei were visualized using DNA Hoechst staining (blue), scale bar = 50 μm. Smurf2WT and Smurf2KdR display similar cellular localization. (**h**) A schematic model showing the link between Smurf2 sumoylation and TGFβ-induced EMT

Discussion

In this study, we have discovered a function for the ubiquitin ligase Smurf2 in the regulation of EMT. Employing 3D cultures of nontransformed mouse mammary epithelial NMuMG cells, knockdown of Smurf2 promotes whereas overexpression of Smurf2 suppresses the ability of TGFβ to induce disruption of acinar morphogenesis of NMuMG cells. We have also found that Smurf2 undergoes sumoylation at Lysines 26 and 369 catalyzed by the SUMO E2 enzyme Ubc9 and the SUMO E3 ligase PIAS3. In mechanistic studies, we have found that sumoylation promotes the ability of Smurf2 to induce the degradation of TβRI and thereby suppresses TGFβ-induced EMT. These findings advance our understanding of the mechanisms that regulate EMT.

Recent studies have shown that TGFβ-induced EMT is regulated by diverse set of post-translational modifications including phosphorylation and ubiquitination.[53,58–62] Phosphorylation of specific serine residues of the transcriptional regulator Twist1 activates EMT and cancer metastasis,

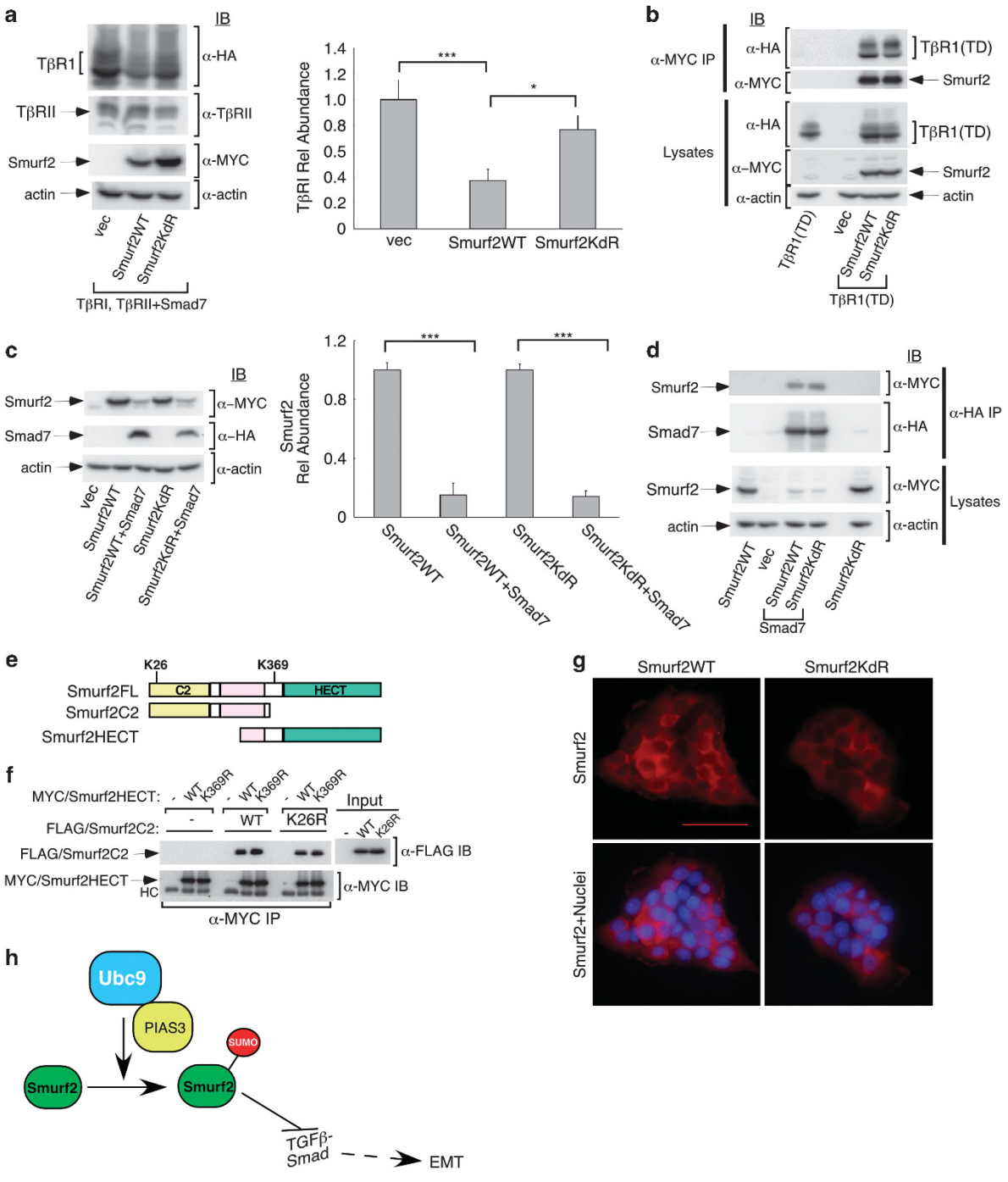

whereas ubiquitin-mediated degradation of Smads inhibits these processes.[18,63,64] In other studies, we have found that sumoylation of the transcriptional regulator SnoN suppresses TGFβ-induced EMT.[40,65] In view of our new findings that Smurf2 suppresses TGFβ-induced EMT, these studies suggest a pivotal role of sumoylation in the regulation of EMT.

Besides undergoing sumoylation, Smurf2 is autoubiquitinated and consequently degraded by the proteasome.[44] Both sumoylation and ubiquitination target specific lysine residues, raising the question of whether and how sumoylation and ubiquitination of Smurf2 might be coordinated. Notably, in our analyses we found no appreciable differences in the abundance of WT and SUMO loss-of-function Smurf2. Consistently, we have found that conversion of the lysine SUMO acceptor sites to arginine in Smurf2 does not significantly affect Smad7-dependent downregulation of Smurf2. In addition, our findings suggest that the lysine to arginine SUMO sites conversion within Smurf2 does not affect Smurf2 association with its adaptor Smad7, and presumably its cognate E2. These observations suggest that distinct lysine residues within Smurf2 are targeted by the SUMO and ubiquitination pathways.

Our study also reveals a mechanism by which sumoylated Smurf2 suppresses EMT. Sumoylation enhances the ability of Smurf2 to induce the degradation of TβRI, explaining how sumoylated Smurf2 opposes the actions of TGFβ signaling in EMT. In future studies, it will be interesting to determine whether sumoylation regulates the ability of Smurf2 to regulate other pathways besides the canonical TGFβ-Smad signaling pathway to control EMT.

Smurf2 regulates diverse biological processes in mitotic and postmitotic cells besides EMT. Smurf2 promotes senescence in fibroblasts, whereas in the nervous system Smurf2 may induce neuronal differentiation and promote neuronal polarization.[66–68] Whether sumoylation contributes to biological responses of Smurf2 besides EMT will be important to investigate in future studies.

TGFβ-induced EMT plays an important role in regulating normal tissue morphogenesis during development as well as cancer invasiveness and metastasis in adults. Our findings that Smurf2 suppresses TGFβ-induced EMT in a sumoylation-dependent manner raises the fundamental question of whether this novel link regulates normal epithelial tissue morphogenesis and affects invasiveness and metastasis of epithelial tumors.

Materials and Methods

Plasmids. CMV-based mammalian expression plasmids containing cDNA encoding MYC-tagged Smurf2 (MYC/Smurf2), HA/SUMO, HA/Ubc9, TβRI/HA, TβRII/HIS, Smad7, FLAG/Smad2, and FLAG/Smad3 proteins have been previously described.[14,15,35,45] Human Smurf2 (K26R), (K369R), and (KdR) in which Lysines 26 and 369, singly or together, are replaced with arginine were generated using a PCR-based site-directed mutagenesis method.[45,65] Vectors containing cDNA to express Smurf2C2 or Smurf2HECT domains harboring WT or Lysine 26 to arginine or Lysine 369 to arginine were generated using PCR-based mutagenesis and subcloning approaches (Figures 8e and f).[69,70] Expression vectors expressing fusion proteins of *Renilla* luciferase (Rluc) with WT or KdR Smurf2 were generated by PCR-based amplification and subcloning of the Rluc cDNA upstream of Smurf2 cDNA in CMV-based (pCMV5B) Smurf2-expression vectors.[14,69,70,71] Smurf2 RNAi vectors encoding Smurf2 hairpin RNAs targeting one of two distinct regions in Smurf2 (5′-GGGCCAAATGACAATGATACA-3′ (Smurf2i-1) and 5′-GGGAAGT CAATTACCTTGGAT-3′ (Smurf2i-2)) and enhanced green fluorescent protein (EGFP) under the control of the U6 and CMV promoters were cloned as previously described.[72,73] RNAi-resistant Smurf2 plasmids Smurf2(r1) and Smurf2(r2) were generated by mutating the Smurf2 cDNA corresponding to the RNAi-1 and RNAi-2 target regions.[70,73] The plasmids were confirmed by DNA sequence analyses (University of Calgary Core Sequencing Facility, Calgary, AB, Canada). The Smad2 and Smad3 RNAi vectors[74,75] and the FLAG/SENP1 and FLAG/SENP2 expression plasmids were kind gifts from Dr. Azad Bonni (Washington University School of Medicine St. Louis, MO, USA). To establish NMuMG stable cell lines, a pCaGip vector was employed to generate constructs containing cDNA encoding WT Smurf2 or a SUMO loss-of-function (KdR) Smurf2 protein. A feature of this vector is that the puromycin resistance marker and protein of interest are encoded by a bicistronic transcript containing Internal Ribosomal Entry Site (IRES).[65,69]

Cell lines and transfections. Human kidney epithelial 293T cells were cultured in Dulbecco's modified Eagle's medium with high glucose and L-glutamine (Invitrogen, Burlington, ON, Canada) supplemented with 10% fetal bovine serum (FBS, Invitrogen). The NAMRU mouse mammary gland epithelial cells (NMuMG), purchased from American Type Culture Collection (ATCC, Manassas, VA, USA), were maintained in Dulbecco's modified Eagle's medium with high glucose and L-glutamine, supplemented with 10 mg/ml insulin and 10% fetal bovine serum. The 293T cells were transiently transfected using the calcium phosphate precipitation method, whereas NMuMG cells were transfected using Lipofectamine LTX Plus reagents (Thermo Fisher Scientific, Life Technologies Inc., Burlington, ON, Canada). NMuMG cells were transfected with pCaGip vector control or one encoding Smurf2 WT or Smurf2KdR using Lipofectamine LTX Plus reagents and incubation in 2 μg/ml puromycin.[45,65,69]

The *in vivo* sumoylation assays, coimmunoprecipitation and immunoblotting. For *in vivo* sumoylation assays, cells were lysed in TNTE (50 mM Tris, 150 mM NaCl, and 1 mM EDTA) buffer containing 0.5% Triton X-100 along with protease and phosphatase inhibitors, and 0.1% SDS.[69,73,76] In addition, 20 mM NEM isopeptidase inhibitor was included in the lysis buffer where indicated.[45,65] Cell extracts were collected in 1.75 ml Eppendorf tubes and centrifuged at 14 000 × *g* for 10 min at 4 °C. Supernatants of cell lysates were collected and subjected to mouse Smurf2 (Santa Cruz Biotechnology, Dallas, TX, USA), mouse anti-MYC (Covance, Burlington, ON, Canada), or mouse anti-FLAG (Sigma-Aldrich, St. Louis, MO, USA) immunoprecipitation at 4 °C, after saving 10% of the supernatant for protein quantification and protein expression analysis.[14,77,78] Immunoprecipitated protein and total protein complexes were resolved by SDS-PAGE, followed by transfer to nitrocellulose membranes, and probing using specific antibodies as previously indicated.[45,65,69,79] For coimmunoprecipitation analyses, cells were lysed in TNTE (50 mM Tris, 150 mM NaCl, and 1 mM EDTA) buffer containing 0.5% Triton X-100 along with protease and phosphatase inhibitors and subjected to immunoprecipitation using mouse anti-HA (Biolegend, Burlington, ON, Canada), rabbit anti-HA (Santa Cruz Biotechnology, Figure 8d), mouse anti-MYC, or mouse anti-FLAG antibody followed by immunoblotting with specific antibodies as indicated. Cell lysates were subjected to mouse anti-actin (Santa Cruz Biotechnology) and used as loading control.

Three-dimensional NMuMG cell formation assay. The nontransformed mouse mammary epithelial NMuMG cells, transiently or stably expressing the indicated proteins, were trypsinized and prepared for 3D culture.[40] Briefly, 75 μl of ice-cold 30% growth factor-reduced Matrigel solution (3 mg/ml final concentration) in growth medium containing antibiotics and antimitotic agents was added to each well of an 8-well chamber slides (Millipore, Billerica, MA, USA). The chamber slides were kept at 37 °C in a 5% CO_2 incubator for 1 h to allow the Matrigel cushions to set. Next, 75 μl of 1.3×10^4 cells/ml of trypsinized and resuspended NMuMG cells in 30% growth factor-reduced Matrigel-containing growth medium was layered on top of the Matrigel cushion in each well of the 8-well chambers, and kept in a controlled 5% CO_2 humidified incubator at 37 °C. The next day, the 3D cell cultures were incubated in the presence or absence of 100 pM TGFβ for 10 days, replenishing the ligand every 3 days. Differential interference contrast (DIC) images of the live 10-day-old NMuMG cellular acini were obtained using an inverted microscope with a 20X objective lens (Olympus IX70, Olympus Canada Inc., Richmond Hill, ON, Canada). The multicellular structures were then fixed with 4% paraformaldehyde, followed by permeabilization using 0.5% cold Triton X-100 solution and blocking using 5% BSA in phosphate-buffered saline. These acini were subjected to immunocytochemical analyses using a rabbit E-cadherin antibody (Cell Signaling

Technology, Whitby, ON, Canada) as the primary antibody and Cy3-conjugated anti-rabbit IgG (Jackson Lab, Burlington, ON, Canada) as the secondary antibody along with the DNA dye bisbenzimide (Hoechst 33258, Invitrogen) to visualize nuclei. Immunofluorescent images of the multicellular colonies were captured using a fluorescent microscope with a 40× objective lens (Zeiss Axiovert 200M, Toronto, ON, Canada). Exposure times for E-cadherin and Hoechst-specific signals were kept constant in each experiment. For each condition, 6 to 10 colonies per experiment were assessed.[40]

Statistical analyses. All data were subjected to statistical analysis by *t*-test or ANOVA followed by Student–Newman–Keuls test (InStat, San Diego, CA, USA). Values of $P<0.05$ were considered statistically significant. $^{*}P<0.05$, $^{**}P<0.01$, and $^{***}P<0.001$. Data were presented graphically as mean ± S.E.M. from experiments that were repeated at least three independent times.

Conflict of Interest

The authors declare no conflict of interest.

Acknowledgements. We thank Dr. Azad Bonni for reagents and discussion and critical reading of the manuscript. This work was supported by grants from the Canadian Institutes of Health Research, Alberta Innovates Health Solutions, and Canadian Breast Cancer Foundation Prairies/NWT to SB, and an Alberta Cancer Foundation Graduate Studentship, a Queen Elizabeth II Graduate Studentship, and an Arnie Charbonneau Cancer Institute Trainee Research Award to ASC.

1. Kalluri R, Neilson EG. Epithelial-mesenchymal transition and its implications for fibrosis. *J Clin Invest* 2003; **112**: 1776–1784.
2. Boyer AS, Ayerinskas II, Vincent EB, McKinney LA, Weeks DL, Runyan RB. TGFbeta2 and TGFbeta3 have separate and sequential activities during epithelial-mesenchymal cell transformation in the embryonic heart. *Dev Biol* 1999; **208**: 530–545.
3. Thiery JP. Epithelial-mesenchymal transitions in tumour progression. *Nat Rev Cancer* 2002; **2**: 442–454.
4. Jakowlew SB. Transforming growth factor-beta in cancer and metastasis. *Cancer Metastasis Rev* 2006; **25**: 435–457.
5. Kang Y, Massague J. Epithelial-mesenchymal transitions: twist in development and metastasis. *Cell* 2004; **118**: 277–279.
6. Thiery JP, Acloque H, Huang RY, Nieto MA. Epithelial-mesenchymal transitions in development and disease. *Cell* 2009; **139**: 871–890.
7. Rotin D, Kumar S. Physiological functions of the HECT family of ubiquitin ligases. *Nat Rev Mol Cell Biol* 2009; **10**: 398–409.
8. Hershko A, Ciechanover A. The ubiquitin system. *Annu Rev Biochem* 1998; **67**: 425–479.
9. Yang Q, Lin HY, Wang HX, Zhang H, Zhang X, Wang HM *et al.* Expression of Smad ubiquitin regulatory factor 2 (Smurf2) in rhesus monkey endometrium and placenta during early pregnancy. *J Histochem Cytochem* 2007; **55**: 453–460.
10. Cao S, Xiao L, Rao JN, Zou T, Liu L, Zhang D *et al.* Inhibition of Smurf2 translation by miR-322/503 modulates TGF-beta/Smad2 signaling and intestinal epithelial homeostasis. *Mol Biol Cell* 2014; **25**: 1234–1243.
11. Narimatsu M, Bose R, Pye M, Zhang L, Miller B, Ching P *et al.* Regulation of planar cell polarity by Smurf ubiquitin ligases. *Cell* 2009; **137**: 295–307.
12. Schwamborn JC, Khazaei MR, Puschel AW. The interaction of mPar3 with the ubiquitin ligase Smurf2 is required for the establishment of neuronal polarity. *J Biol Chem* 2007; **282**: 35259–35268.
13. Podos SD, Hanson KK, Wang YC, Ferguson EL. The DSmurf ubiquitin-protein ligase restricts BMP signaling spatially and temporally during Drosophila embryogenesis. *Dev Cell* 2001; **1**: 567–578.
14. Bonni S, Wang HR, Causing CG, Kavsak P, Stroschein SL, Luo K *et al.* TGF-beta induces assembly of a Smad2-Smurf2 ubiquitin ligase complex that targets SnoN for degradation. *Nat Cell Biol* 2001; **3**: 587–595.
15. Stroschein SL, Bonni S, Wrana JL, Luo K. Smad3 recruits the anaphase-promoting complex for ubiquitination and degradation of SnoN. *Genes Dev* 2001; **15**: 2822–2836.
16. Tang Y, Liu Z, Zhao L, Clemens TL, Cao X. Smad7 stabilizes beta-catenin binding to E-cadherin complex and promotes cell-cell adhesion. *J Biol Chem* 2008; **283**: 23956–23963.
17. Tang LY, Yamashita M, Coussens NP, Tang Y, Wang X, Li C *et al.* Ablation of Smurf2 reveals an inhibition in TGF-beta signalling through multiple mono-ubiquitination of Smad3. *EMBO J* 2011; **30**: 4777–4789.
18. Inoue Y, Imamura T. Regulation of TGF-beta family signaling by E3 ubiquitin ligases. *Cancer Sci* 2008; **99**: 2107–2112.
19. Fukunaga E, Inoue Y, Komiya S, Horiguchi K, Goto K, Saitoh M *et al.* Smurf2 induces ubiquitin-dependent degradation of Smurf1 to prevent migration of breast cancer cells. *J Biol Chem* 2008; **283**: 35660–35667.
20. Kim S, Jho EH. The protein stability of Axin, a negative regulator of Wnt signaling, is regulated by Smad ubiquitination regulatory factor 2 (Smurf2). *J Biol Chem* 2010; **285**: 36420–36426.
21. Cai Y, Shen XZ, Zhou CH, Wang JY. Abnormal expression of Smurf2 during the process of rat liver fibrosis. *Chin J Dig Dis* 2006; **7**: 237–245.
22. Cai Y, Zhou CH, Fu D, Shen XZ. Overexpression of Smad ubiquitin regulatory factor 2 suppresses transforming growth factor-beta mediated liver fibrosis. *J Dig Dis* 2012; **13**: 327–334.
23. Lin X, Liang M, Feng XH. Smurf2 is a ubiquitin E3 ligase mediating proteasome-dependent degradation of Smad2 in transforming growth factor-beta signaling. *J Biol Chem* 2000; **275**: 36818–36822.
24. Geiss-Friedlander R, Melchior F. Concepts in sumoylation: a decade on. *Nat Rev Mol Cell Biol* 2007; **8**: 947–956.
25. Johnson ES. Protein modification by SUMO. *Annu Rev Biochem* 2004; **73**: 355–382.
26. Yeh ET. SUMOylation and De-SUMOylation: wrestling with life's processes. *J Biol Chem* 2009; **284**: 8223–8227.
27. Massague J. TGFbeta in cancer. *Cell* 2008; **134**: 215–230.
28. Valdes F, Alvarez AM, Locascio A, Vega S, Herrera B, Fernandez M *et al.* The epithelial mesenchymal transition confers resistance to the apoptotic effects of transforming growth factor Beta in fetal rat hepatocytes. *Mol Cancer Res* 2002; **1**: 68–78.
29. Polyak K, Weinberg RA. Transitions between epithelial and mesenchymal states: acquisition of malignant and stem cell traits. *Nat Rev Cancer* 2009; **9**: 265–273.
30. Derynck R, Akhurst RJ. Differentiation plasticity regulated by TGF-beta family proteins in development and disease. *Nat Cell Biol* 2007; **9**: 1000–1004.
31. Siegel PM, Massague J. Cytostatic and apoptotic actions of TGF-beta in homeostasis and cancer. *Nat Rev Cancer* 2003; **3**: 807–821.
32. Ozdamar B, Bose R, Barrios-Rodiles M, Wang HR, Zhang Y, Wrana JL. Regulation of the polarity protein Par6 by TGFbeta receptors controls epithelial cell plasticity. *Science* 2005; **307**: 1603–1609.
33. Valcourt U, Kowanetz M, Niimi H, Heldin CH, Moustakas A. TGF-beta and the Smad signaling pathway support transcriptomic reprogramming during epithelial-mesenchymal cell transition. *Mol Biol Cell* 2005; **16**: 1987–2002.
34. Di Guglielmo GM, Le Roy C, Goodfellow AF, Wrana JL. Distinct endocytic pathways regulate TGF-beta receptor signalling and turnover. *Nat Cell Biol* 2003; **5**: 410–421.
35. Kavsak P, Rasmussen RK, Causing CG, Bonni S, Zhu H, Thomsen GH *et al.* Smad7 binds to Smurf2 to form an E3 ubiquitin ligase that targets the TGF beta receptor for degradation. *Mol Cell* 2000; **6**: 1365–1375.
36. Miettinen PJ, Ebner R, Lopez AR, Derynck R. TGF-beta induced transdifferentiation of mammary epithelial cells to mesenchymal cells: involvement of type I receptors. *J Cell Biol* 1994; **127**(6 Pt 2): 2021–2036.
37. Peng SB, Yan L, Xia X, Watkins SA, Brooks HB, Beight D *et al.* Kinetic characterization of novel pyrazole TGF-beta receptor I kinase inhibitors and their blockade of the epithelial-mesenchymal transition. *Biochemistry* 2005; **44**: 2293–2304.
38. Debnath J, Brugge JS. Modelling glandular epithelial cancers in three-dimensional cultures. *Nat Rev Cancer* 2005; **5**: 675–688.
39. Swamydas M, Eddy JM, Burg KJ, Dreau D. Matrix compositions and the development of breast acini and ducts in 3D cultures. *In Vitro Cell Dev Biol Anim* 2010; **46**: 673–684.
40. Ikeuchi Y, Dadakhujaev S, Chandhoke AS, Huynh MA, Oldenborg A, Ikeuchi M *et al.* TIF1gamma protein regulates epithelial-mesenchymal transition by operating as a small ubiquitin-like modifier (SUMO) E3 ligase for the transcriptional regulator SnoN1. *J Biol Chem* 2014; **289**: 25067–25078.
41. Shaw KR, Wrobel CN, Brugge JS. Use of three-dimensional basement membrane cultures to model oncogene-induced changes in mammary epithelial morphogenesis. *J Mammary Gland Biol Neoplasia* 2004; **9**: 297–310.
42. Godde NJ, Galea RC, Elsum IA, Humbert PO. Cell polarity in motion: redefining mammary tissue organization through EMT and cell polarity transitions. *J Mammary Gland Biol Neoplasia* 2010; **15**: 149–168.
43. Moreno-Bueno G, Peinado H, Molina P, Olmeda D, Cubillo E, Santos V *et al.* The morphological and molecular features of the epithelial-to-mesenchymal transition. *Nat Protoc* 2009; **4**: 1591–1613.
44. Wiesner S, Ogunjimi AA, Wang HR, Rotin D, Sicheri F, Wrana JL *et al.* Autoinhibition of the HECT-type ubiquitin ligase Smurf2 through its C2 domain. *Cell* 2007; **130**: 651–662.
45. Hsu YH, Sarker KP, Pot I, Chan A, Netherton SJ, Bonni S. Sumoylated SnoN represses transcription in a promoter-specific manner. *J Biol Chem* 2006; **281**: 33008–33018.
46. Matunis MJ, Coutavas E, Blobel G. A novel ubiquitin-like modification modulates the partitioning of the Ran-GTPase-activating protein RanGAP1 between the cytosol and the nuclear pore complex. *J Cell Biol* 1996; **135**(6 Pt 1): 1457–1470.
47. Suzuki T, Ichiyama A, Saitoh H, Kawakami T, Omata M, Chung CH *et al.* A new 30-kDa ubiquitin-related SUMO-1 hydrolase from bovine brain. *J Biol Chem* 1999; **274**: 31131–31134.
48. Pichler A, Gast A, Seeler JS, Dejean A, Melchior F. The nucleoporin RanBP2 has SUMO1 E3 ligase activity. *Cell* 2002; **108**: 109–120.
49. Gong L, Kamitani T, Fujise K, Caskey LS, Yeh ET. Preferential interaction of sentrin with a ubiquitin-conjugating enzyme, Ubc9. *J Biol Chem* 1997; **272**: 28198–28201.

50. Palvimo JJ. PIAS proteins as regulators of small ubiquitin-related modifier (SUMO) modifications and transcription. *Biochem Soc Trans* 2007; **35**(Pt 6): 1405–1408.
51. Kotaja N, Karvonen U, Janne OA, Palvimo JJ. PIAS proteins modulate transcription factors by functioning as SUMO-1 ligases. *Mol Cell Biol* 2002; **22**: 5222–5234.
52. Hickey CM, Wilson NR, Hochstrasser M. Function and regulation of SUMO proteases. *Nat Rev Mol Cell Biol* 2012; **13**: 755–766.
53. Shi Y, Massague J. Mechanisms of TGF-beta signaling from cell membrane to the nucleus. *Cell* 2003; **113**: 685–700.
54. Zavadil J, Bottinger EP. TGF-beta and epithelial-to-mesenchymal transitions. *Oncogene* 2005; **24**: 5764–5774.
55. Miyazono K. Transforming growth factor-beta signaling in epithelial-mesenchymal transition and progression of cancer. *Proc Jp Acad Ser B Phys Biol Sci* 2009; **85**: 314–323.
56. Ogunjimi AA, Briant DJ, Pece-Barbara N, Le Roy C, Di Guglielmo GM, Kavsak P *et al.* Regulation of Smurf2 ubiquitin ligase activity by anchoring the E2 to the HECT domain. *Mol Cell* 2005; **19**: 297–308.
57. Izzi L, Attisano L. Regulation of the TGFbeta signalling pathway by ubiquitin-mediated degradation. *Oncogene* 2004; **23**: 2071–2078.
58. Galliher AJ, Schiemann WP. Beta3 integrin and Src facilitate transforming growth factor-beta mediated induction of epithelial-mesenchymal transition in mammary epithelial cells. *Breast Cancer Res* 2006; **8**: R42.
59. Galliher AJ, Schiemann WP. Src phosphorylates Tyr284 in TGF-beta type II receptor and regulates TGF-beta stimulation of p38 MAPK during breast cancer cell proliferation and invasion. *Cancer Res* 2007; **67**: 3752–3758.
60. Kwon A, Lee HL, Woo KM, Ryoo HM, Baek JH. SMURF1 plays a role in EGF-induced breast cancer cell migration and invasion. *Mol Cells* 2013; **36**: 548–555.
61. Park SH, Jung EH, Kim GY, Kim BC, Lim JH, Woo CH. Itch E3 ubiquitin ligase positively regulates TGF-beta signaling to EMT via Smad7 ubiquitination. *Mol Cell* 2014; **38**: 20–25.
62. Yamashita M, Fatyol K, Jin C, Wang X, Liu Z, Zhang YE. TRAF6 mediates Smad-independent activation of JNK and p38 by TGF-beta. *Mol Cell* 2008; **31**: 918–924.
63. Hong J, Zhou J, Fu J, He T, Qin J, Wang L *et al.* Phosphorylation of serine 68 of Twist1 by MAPKs stabilizes Twist1 protein and promotes breast cancer cell invasiveness. *Cancer Res* 2011; **71**: 3980–3990.
64. Zhang Y, Chang C, Gehling DJ, Hemmati-Brivanlou A, Derynck R. Regulation of Smad degradation and activity by Smurf2, an E3 ubiquitin ligase. *Proc Natl Acad Sci USA* 2001; **98**: 974–979.
65. Netherton SJ, Bonni S. Suppression of TGFbeta-induced epithelial-mesenchymal transition like phenotype by a PIAS1 regulated sumoylation pathway in NMuMG epithelial cells. *PLoS One* 2010; **5**: e13971.
66. Kong Y, Cui H, Zhang H. Smurf2-mediated ubiquitination and degradation of Id1 regulates p16 expression during senescence. *Aging Cell* 2011; **10**: 1038–1046.
67. Yu YL, Chou RH, Shyu WC, Hsieh SC, Wu CS, Chiang SY *et al.* Smurf2-mediated degradation of EZH2 enhances neuron differentiation and improves functional recovery after ischaemic stroke. *EMBO Mol Med* 2013; **5**: 531–547.
68. Zhang H, Cohen SN. Smurf2 up-regulation activates telomere-dependent senescence. *Genes Dev* 2004; **18**: 3028–3040.
69. Pot I, Patel S, Deng L, Chandhoke AS, Zhang C, Bonni A *et al.* Identification of a novel link between the protein kinase NDR1 and TGFbeta signaling in epithelial cells. *PLoS One* 2013; **8**: e67178.
70. Huynh MA, Ikeuchi Y, Netherton S, de la Torre-Ubieta L, Kanadia R, Stegmuller J *et al.* An isoform-specific SnoN1-FOXO1 repressor complex controls neuronal morphogenesis and positioning in the mammalian brain. *Neuron* 2011; **69**: 930–944.
71. Stroschein SL, Wang W, Zhou S, Zhou Q, Luo K. Negative feedback regulation of TGF-beta signaling by the SnoN oncoprotein. *Science* 1999; **286**: 771–774.
72. Konishi Y, Stegmuller J, Matsuda T, Bonni S, Bonni A. Cdh1-APC controls axonal growth and patterning in the mammalian brain. *Science* 2004; **303**: 1026–1030.
73. Sarker KP, Wilson SM, Bonni S. SnoN is a cell type-specific mediator of transforming growth factor-beta responses. *J Biol Chem* 2005; **280**: 13037–13046.
74. Bernard DJ. Both SMAD2 and SMAD3 mediate activin-stimulated expression of the follicle-stimulating hormone beta subunit in mouse gonadotrope cells. *Mol Endocrinol* 2004; **18**: 606–623.
75. Stegmuller J, Huynh MA, Yuan Z, Konishi Y, Bonni A. TGFbeta-Smad2 signaling regulates the Cdh1-APC/SnoN pathway of axonal morphogenesis. *J Neurosci* 2008; **28**: 1961–1969.
76. Dadakhujaev S, Salazar-Arcila C, Netherton SJ, Chandhoke AS, Singla AK, Jirik FR *et al.* A novel role for the SUMO E3 ligase PIAS1 in cancer metastasis. *Oncoscience* 2014; **1**: 229–240.
77. Macias-Silva M, Abdollah S, Hoodless PA, Pirone R, Attisano L, Wrana JL. MADR2 is a substrate of the TGFbeta receptor and its phosphorylation is required for nuclear accumulation and signaling. *Cell* 1996; **87**: 1215–1224.
78. Abdollah S, Macias-Silva M, Tsukazaki T, Hayashi H, Attisano L, Wrana JL. TbetaRI phosphorylation of Smad2 on Ser465 and Ser467 is required for Smad2-Smad4 complex formation and signaling. *J Biol Chem* 1997; **272**: 27678–27685.
79. Eapen SA, Netherton SJ, Sarker KP, Deng L, Chan A, Riabowol K *et al.* Identification of a novel function for the chromatin remodeling protein ING2 in muscle differentiation. *PLoS One* 2012; **7**: e40684.

Supplementary Information accompanies this paper on Cell Death and Differentiation website (http://www.nature.com/cdd)